Revista Mexicana de Astronomía y Astrofísica, **37**, 15–33 (2001)

CCD UBVI PHOTOMETRY AND POLARIMETRY IN THE OPEN CLUSTER TRUMPLER 21[1]

E. E. Giorgi,[2] G. Baume,[3] R. A. Vázquez,[4] and A. Feinstein[4]

Received 1999 June 8; accepted 2000 November 22

RESUMEN

Se realizó fotometría CCD *UBVI* en el campo del cúmulo abierto Trumpler 21. Nuestros datos ubican al cúmulo a una distancia de 1380 pc en una zona de baja absorción con $E(B-V) = 0.25$. La edad del cúmulo se estimó entre $25 - 30 \times 10^6$ años basándose en la superposición de isocronas calculadas con pérdida de masa y *overshooting*. El espectro de masas del cúmulo tiene una pendiente de 1.44, similar al valor típico 1.35 para estrellas de campo. A partir de polarimetría *UBVRI* de sus miembros más brillantes se encontró que el material interestelar difuso es responsable tanto del porcentaje de polarización como de su dirección.

ABSTRACT

CCD *UBVI* photometry was carried out in the field of the open cluster Trumpler 21. Our data locate the cluster at a distance of 1380 pc in a low absorption zone with $E(B-V) = 0.25$. The age of the cluster is estimated to be $25-30\times10^6$ yr based on the superposition of isochrones computed with mass loss and overshooting. The cluster mass spectrum has a slope of 1.44 similar to the typical value 1.35 for field stars. *UBVRI* polarimetry of its brightest members led us to the finding that diffuse interstellar material is responsible for both polarization percentage and its direction.

Key Words: **OPEN CLUSTERS AND ASSOCIATIONS: INDIVIDUAL: TRUMPLER 21 — POLARIZATION — STARS: IMAGING — STARS: MASS FUNCTION**

1. INTRODUCTION

Open clusters are of upmost importance to put both stellar evolution theories, and the kinematics and formation of the Galactic disk to the test. Quite often, however, small and sparse open clusters are not taken into account, despite being the main source of stellar enrichment. Of particular interest is the way stars form what is called the mass spectrum. Such a study requires an accurate determination of distance and the inclusion of as many faint members as possible, now made easier with high sensitivity CCD detectors.

Trumpler 21 C1328–625 ($\alpha_{2000} = 13^h32^m11^s, \delta_{2000} = -62°47'25''; l = 307°.57, b = -0°.28$) is a small size (5′ diameter) young open cluster located close to the Coalsack in the Centaurus Association. Photoelectric photometry of 17 stars in the field of this cluster was made by Moffat & Vogt (1973; MV73 hereafter), who obtained $< E(B-V) > = 0.21$ and $V_0 - M_V = 10.90$. Later on, Peterson & FitzGerald (1988; PF88 hereafter) extended the observations to 24 stars finding $< E(B-V) > = 0.25$ and $V_0 - M_V = 10.52$. The available spectroscopic information on Trumpler 21 comes from FitzGerald et al. (1979) who observed four stars. Additional spectroscopic information can also be found in Houk, Cowley, & Smith-More (1975). Kumar

[1]Based on observations collected at the University of Toronto Southern Observatory, Las Campanas, Chile, and the Complejo Astronómico El Leoncito, Argentina, operated under agreement of CONICET, and La Plata, Córdoba, and San Juan Universities.
[2]Fellow of Comisión de Investigaciones Científicas de la Provincia de Buenos Aires, Argentina.
[3]Fellow of CONICET.
[4]Member of the Carrera de Investigador Científico, CONICET.

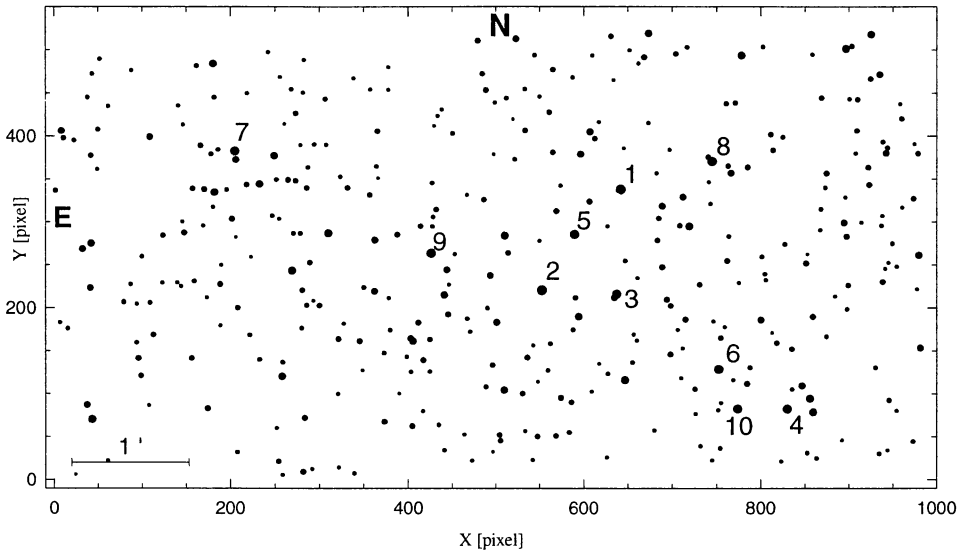

Fig. 1. Finding Chart of Trumpler 21. North and East are indicated. The size of the symbols approximately represents star magnitude. Some stars with numbers from this work are indicated; star #1 coordinates are $\alpha_{2000} = 13^h32^m10^s$, $\delta_{2000} = -62°46'50''$.

(1978) suggested that the supernova remnant G307.6–0.3 is in the cluster Trumpler 21, but this radio source is not included in the Whiteoak & Green's (1996) supernova remnant catalogue.

Our ongoing program on open clusters has been designed to examine their observational parameters such as their distance, color excess, age, and mass spectrum, by including their faint members. The observational procedure to obtain CCD $UBVI$ imaging photometry and $UBVRI$ polarimetry is described in § 2. Section 3 includes the membership analysis and the determination of color excesses. Cluster distance and age, main results from polarimetry, and mass spectrum are discussed in § 4, 5, and 6, respectively.

2. OBSERVATIONS

2.1. CCD *Photometry*

CCD $UBVI$ (Cousins system) imaging photometry was undertaken in the open cluster Trumpler 21 in June 15, 1993. Data were obtained with the 60 cm telescope of the University of Toronto Southern Observatory at Las Campanas Observatory, Chile, and a PM 512 x 512 METACHROME-II UV-coated CCD. The scale of the chip is $0.45''$ pixels^{-1}, thus covering a field of $4'$ on a side. Two overlapping fields, shown in the finding chart of Figure 1, were measured under good seeing conditions ($\approx 1.5''$). Typical exposure times per filter were: from 180 to 1200 seconds in U, from 70 to 700 in B, from 25 to 450 in V, and from 15 to 110 in I. In the U and B bands, two long exposures were taken to improve the statistics of faint stars. Instrumental signatures were removed using bias and sky flat frames. The point spread function (PSF) fitting, using DAOPHOT (Stetson 1987), was used to derive instrumental colors and magnitudes. These values were transformed into the standard system through a set of stars observed in the open cluster NGC 5606 (Vázquez et al. 1994) and with extinction coefficients from Grotues & Gocherman (1992). The accuracy of the calibration is ≈ 0.03 mag (rms) in all the bands.

Table 1 lists the photometry output for 366 stars. It includes: identification numbers, numbers from PF88, x and y coordinates, magnitudes and colors, and comments on the membership. We want to remark that this table shows a group of stars without $(U - B)$ colors because the long exposure frames in the U filter were not long enough to reach the same magnitude limit achieved in the BVI frames. Three stars not included in our survey but formerly observed by PF88 were added to our data since they are of crucial importance in the

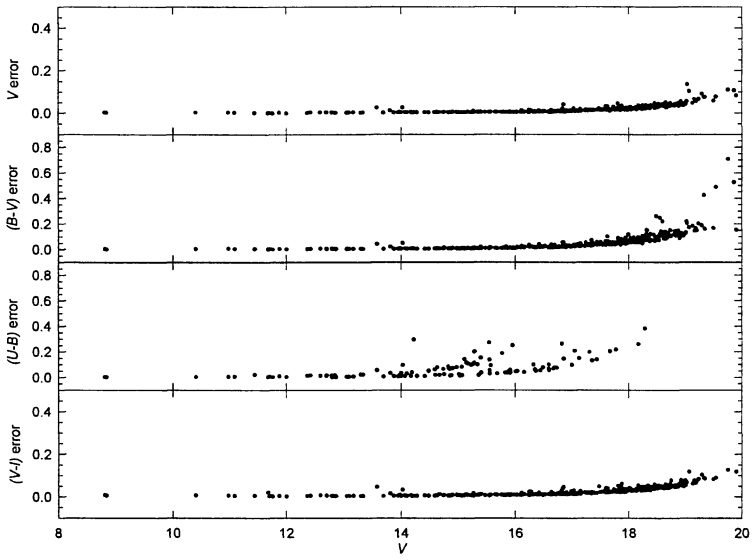

Fig. 2. Color and magnitude errors against V magnitude.

determination of the cluster mass spectrum (see § 6, ahead); they are # 20, # 22, and # 23 in PF88 notation. For the sake of completeness, Figure 2 shows the path of error values for colors and magnitudes, as given by DAOPHOT, against the magnitude V.

The average differences between our photometry and the previous studies of MV73 and PF88 (in the sense: our values minus other authors') are indicated in Table 2. There is a good agreement with PF88 photometry but a large systematic difference $\Delta V = 0.08$ appears when compared with MV73 measurements. In general, all our indices are slightly bluer than the ones from PF88 and MV73, but we do not see a compelling reason to correct our data.

TABLE 2

COMPARISON OF OUR PHOTOMETRY WITH OTHER PAPERS [a]

Author	$< \Delta V >$	$< \Delta(B-V) >$	$< \Delta(U-B) >$
PF88	-0.011 ± 0.031	-0.025 ± 0.010	-0.018 ± 0.015
MV73	-0.081 ± 0.009	-0.010 ± 0.009	-0.052 ± 0.007

[a] Standard deviations are indicated.

2.2. *Polarization Measurements*

Polarimetric data for 13 stars were obtained with the Torino Observatory Five Channel Photopolarimeter, attached to the 215 cm telescope of the Complejo Astronómico El Leoncito (CASLEO), in two observational runs in May 1 and May 3, 1998. The observations were made with a $15''$ aperture diaphragm and $UBVRI$ filters having effective wavelengths: $\lambda_{U_{eff}} = 0.360$ μm, $\lambda_{B_{eff}} = 0.440$ μm, $\lambda_{V_{eff}} = 0.530$ μm, $\lambda_{R_{eff}} = 0.690$ μm, and $\lambda_{I_{eff}} = 0.830$ μm. Standard stars with 0% polarization (HD 68456, HD 102365, and HD 146233), from Gliese (1969) and with 0° of polarization angle (HD 111613, HD 147084, and HD 187929; Serkowski, Mathewson, & Ford 1975) were observed each night. The star identification, the number of measurements n, the percentage of polarization P_λ, the position angle θ_λ and the corresponding errors for each filter are included in Table 3. The

TABLE 3
POLARIZATION MEASUREMENTS

Star	Filter	P[%]	θ[deg]	Star	Filter	P[%]	θ[deg]
1	U	1.06 ± 0.07	73.3 ± 2.0	8	U	1.25 ± 0.05	73.3 ± 1.1
(n=5)	B	1.18 ± 0.07	78.9 ± 1.7	(n=4)	B	1.26 ± 0.05	79.0 ± 1.1
	V	1.21 ± 0.05	80.3 ± 1.1		V	1.41 ± 0.04	78.0 ± 0.9
	R	1.26 ± 0.03	78.7 ± 0.7		R	1.29 ± 0.04	
	I	1.30 ± 0.08	80.5 ± 1.8		I	1.22 ± 0.06	79.8 ± 1.4
$\lambda_{max}[\mu m]$	0.601 ± 0.036			$\lambda_{max}[\mu m]$	0.538 ± 0.023		
P_{max}[%]	1.29 ± 0.04			P_{max}[%]	1.41 ± 0.04		
2	U	1.04 ± 0.09	80.0 ± 2.5	9	U	1.18 ± 0.13	78.0 ± 3.2
(n=4)	B	1.06 ± 0.06	78.1 ± 1.5	(n=4)	B	1.38 ± 0.04	80.5 ± 0.8
	V	1.30 ± 0.07	82.1 ± 1.5		V	1.09 ± 0.04	82.4 ± 1.0
	R	1.19 ± 0.04	82.8 ± 1.1		R	1.10 ± 0.06	82.8 ± 1.7
	I	1.31 ± 0.14	74.2 ± 3.2		I	1.08 ± 0.06	83.5 ± 1.6
$\lambda_{max}[\mu m]$	0 .594 ± 0.040			$\lambda_{max}[\mu m]$	0.477 ± 0.068		
P_{max}[%]	1.25 ± 0.05			P_{max}[%]	1.28 ± 0.09		
3	U	1.12 ± 0.09	70.3 ± 2.3	19	U	1.63 ± 0.25	56.3 ± 4.4
(n=4)	B	1.11 ± 0.06	69.3 ± 1.7	(n=4)	B	1.51 ± 0.13	72.6 ± 2.4
	V	1.24 ± 0.04	74.8 ± 0.9		V	1.23 ± 0.17	75.1 ± 4.0
	R	1.26 ± 0.03	73.7 ± 0.8		R	1.33 ± 0.10	74.0 ± 2.1
	I	1.04 ± 0.11	72.9 ± 3.0		I	1.14 ± 0.22	78.6 ± 5.6
$\lambda_{max}[\mu m]$	0.584 ± 0.028			$\lambda_{max}[\mu m]$	0.475 ± 0.045		
P_{max}[%]	1.28 ± 0.03			P_{max}[%]	1.51 ± 0.09		
4	U	1.18 ± 0.05	73.8 ± 1.2	20[a]	U	0.59 ± 0.34	62.7 ± 16.4
(n=4)	B	1.19 ± 0.04	76.3 ± 1.0	(n=4)	B	0.64 ± 0.09	78.4 ± 3.9
	V	1.25 ± 0.01	78.1 ± 0.3		V	0.80 ± 0.14	80.9 ± 4.9
	R	1.26 ± 0.01	75.5 ± 0.3		R	0.80 ± 0.09	81.4 ± 3.4
	I	1.00 ± 0.09	76.8 ± 2.7		I	0.26 ± 0.17	11.1 ± 18.7
$\lambda_{max}[\mu m]$	0.573 ± 0.028			$\lambda_{max}[\mu m]$	0.544 ± 0.115		
P_{max}[%]	1.28 ± 0.02			P_{max}[%]	0.73 ± 0.08		
5	U	1.25 ± 0.14	75.8 ± 3.2	22(PF88)	U	1.09 ± 0.08	73.1 ± 2.2
(n=4)	B	1.24 ± 0.12	79.2 ± 2.8	(n=4)	B	1.04 ± 0.03	75.0 ± 0.7
	V	1.78 ± 0.16	80.0 ± 2.5		V	0.79 ± 0.05	77.9 ± 1.8
	R	1.42 ± 0.14	82.2 ± 2.7		R	0.93 ± 0.10	73.7 ± 3.1
	I	1.35 ± 0.34	85.8 ± 7.3		I	0.93 ± 0.09	72.6 ± 2.7
$\lambda_{max}[\mu m]$	0.579 ± 0.063			$\lambda_{max}[\mu m]$	0.451 ± 0.087		
P_{max}[%]	1.54 ± 0.11			P_{max}[%]	1.02 ± 0.07		
6[a]	U	1.04 ± 0.42	89.1 ± 11.7	23(PF88)	U	0.84 ± 0.20	62.7 ± 7.0
(n=4)	B	1.40 ± 0.13	74.0 ± 2.6	(n=4)	B	1.35 ± 0.10	68.5 ± 2.2
	V	1.23 ± 0.04	73.4 ± 1.0		V	1.03 ± 0.07	74.5 ± 1.9
	R	1.13 ± 0.03	74.8 ± 0.8		R	1.37 ± 0.06	68.4 ± 1.3
	I	1.03 ± 0.09	73.1 ± 2.4		I	1.03 ± 0.39	70.3 ± 10.7
$\lambda_{max}[\mu m]$	0.517 ± 0.028			$\lambda_{max}[\mu m]$	0.674 ± 0.131		
P_{max}[%]	1.25 ± 0.04			P_{max}[%]	1.31 ± 0.13		
7	U	0.97 ± 0.10	73.0 ± 3.0				
(n=4)	B	0.86 ± 0.17	71.9 ± 5.8				
	V	1.22 ± 0.08	72.8 ± 1.9				
	R	1.21 ± 0.11	76.2 ± 2.6				
	I	0.79 ± 0.34	55.1 ± 12.2				
$\lambda_{max}[\mu m]$	0.538 ± 0.023						
P_{max}[%]	1.41 ± 0.04						

[a] Stars # 6 and # 20 are foreground stars.

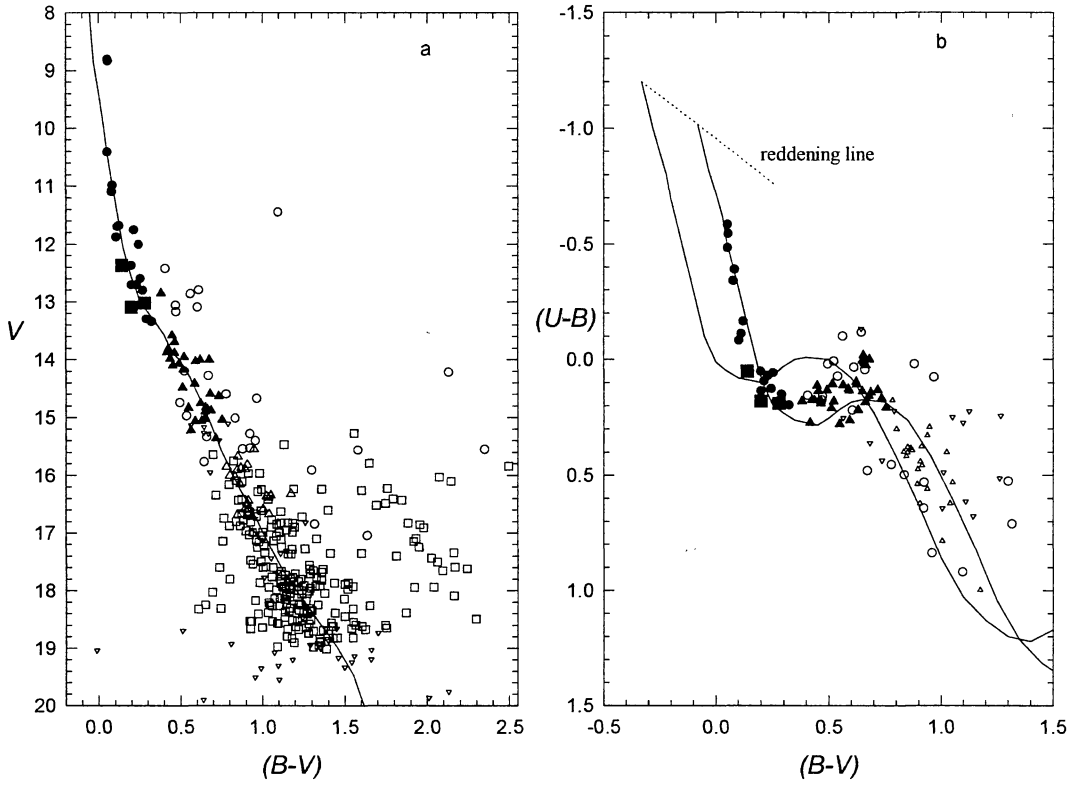

Fig. 3. *a*. The V versus $(B-V)$ diagram. Symbols: filled circles for likely members (filled squares are likely members whose photometry was taken from PF88); filled triangles for probable members; and open circles for non-members. No membership is assigned for the next stars: without $(U-B)$ indices (open squares), with color errors ≤ 0.1 (open triangles) and with color errors ≥ 0.1 (open inverted triangles). The solid line represents the ZAMS (Schmidt-Kaler 1982) fitted to a distance modulus of 11.47 (see § 4). *b*. Color-color diagram; symbols as in Fig. 3*a*. The intrinsic location of the ZAMS and its location after reddening ($E(B-V) = 0.25$) obtained in this study are indicated.

uncertainty of the polarization (ΔP) is obtained from photon statistics. The uncertainty of the polarization angle ($\Delta\theta$) was estimated using the Hsu & Breger's equation (1982)

$$\Delta\theta = 28^{\circ}.65 \times \frac{\Delta P}{P} .$$

As seen in Table 3, the accuracy of the polarization angle is low, especially for stars # 19 and # 6 in the U band. Indeed, more observations should be carried out to achieve a better accuracy in the polarization angle but, for the purpose of determining the general trend of polarization vectors, our data are accurate enough.

3. DATA ANALYSIS

The observed photometry for Trumpler 21 is shown in Figs. 3*a*-*b* and 4*a*-*b* together with the Schmidt-Kaler's (1982) ZAMS and the relation from Cousins (1978). All these diagrams show that the cluster sequence, composed of stars with colors bluer than $(B-V) = 0.7$ and $(U-B) = 0.2$, clearly extends down to $V \approx 15$. Beyond these limits, cluster stars merge into field stars making any membership assessment unrealistic. A fruitless attempt to identify faint cluster members was made inspecting the *Hipparcos* and *Tycho* catalogues data (ESA, 1997). Only three of the stars observed by us are included in this data base: stars # 1, # 2, and # 4 (cluster members from PF88 analysis). Moreover, these stars have such large parallax errors associated that no independent distance estimation of the cluster could be done with them. Thus, because of the lack of proper motion studies and the few available spectroscopic data, membership assessment was based on photometric criteria according to the star location in all the photometric diagrams. This procedure was applied up to

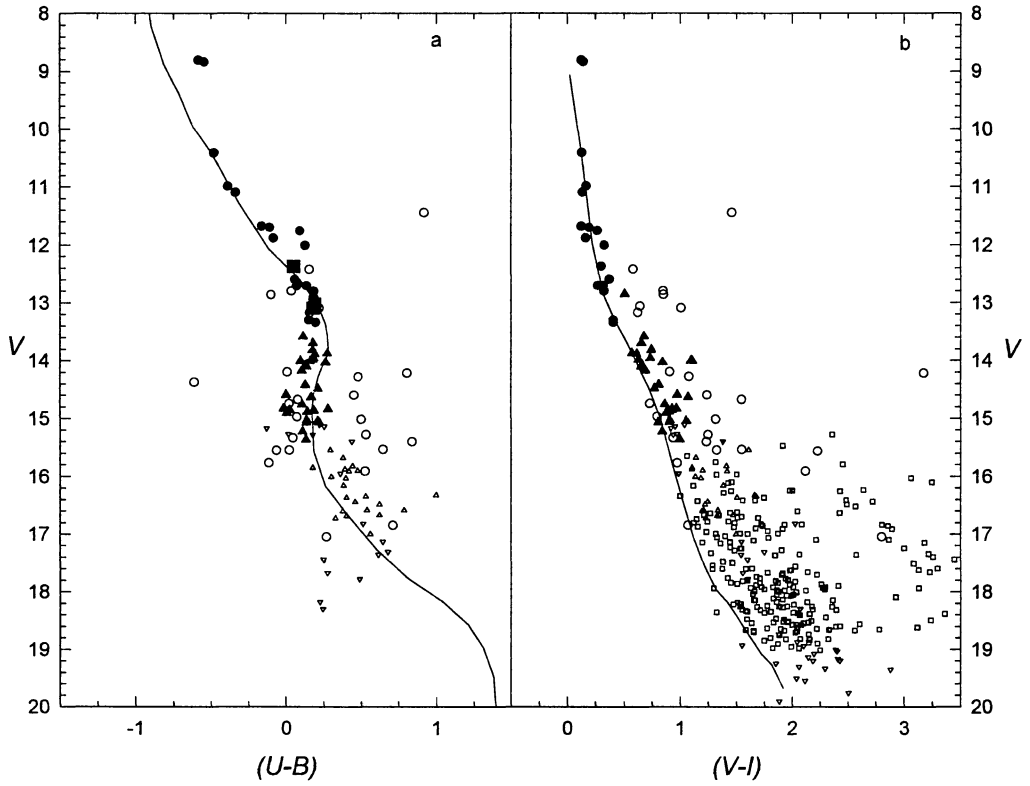

Fig. 4. *a.* The V versus $(U-B)$ diagram. The solid line represents the ZAMS (Schmidt-Kaler 1982); symbols have the same meaning as in Fig. 3*a*. *b.* The V versus $(V-I)$ diagram. The solid line shows the relation for main sequence stars from Cousins (1978); symbols as in Figure 3*a*.

$V \approx 15$. We stated three membership categories: likely members, probable members and non-members. A detail of memberships can be found on Table 1. The four stars with spectral types from FitzGerald et al. (1979), # 1 (HD 117492, B5III), # 2 (HD 117513, B2III), # 3 (B2V), and # 5 (B8V) are likely cluster members. There is a group of stars, however, for which no realistic membership assessment is possible because they either do not have $(U-B)$ indices or cannot be clearly segregated from field stars.

Intrinsic colors of stars with unambiguous reddening solution were individually computed using the procedure explained in Vázquez et al. (1995). From them, mean color excesses $< E(B-V) > = 0.25 \pm 0.02$ and $< E(U-B) > = 0.18$ were derived, in good agreement with PF88. Probable members were de-reddened using these values.

The absorption law towards this cluster was estimated using individual $E(V-I)$ excess of likely cluster members derived through the relation between $(V-I)_0$ and spectral types or between $(B-V)_0$ and $(U-B)_0$ indices according to Cousins (1978). When plotted against $(B-V)$, as shown in Figure 5, they closely follow the $E(V-I)/E(B-V) = 1.24$ ratio predicted by Dean, Warren, & Cousins (1978) for $R = A_V/E(B-V) = 3.1$, for normal absorbing material. Since the extinction law in the direction of Trumpler 21 is normal, absorption free magnitudes were computed as $V_0 = V - 3.1 \times E(B-V)$.

Two features are to be noticed in the magnitude and color diagrams. In Fig. 3*b*, some probable members (filled triangles) having $0.35 < (B-V) < 0.6$ rise above the reddened ZAMS showing $\delta(U-B)$ ultraviolet excess. If our membership assessment is correct, then these stars are serious candidates to be affected by blanketting (Greenstein 1965); however, further investigation is required. On the other side, in Figs. 3*a* and 4*b* there is a group of stars forming a notoriously evident parallel sequence in the magnitude interval $15 < V < 19$. All these stars are marginally concentrated towards the cluster centre and from their locations in the cluster color-magnitude diagrams they could be pre-main sequence stars. However, the magnitude scatter of this parallel sequence, at constant color, is reduced, a fact not favoring this assumption. It would be possible to

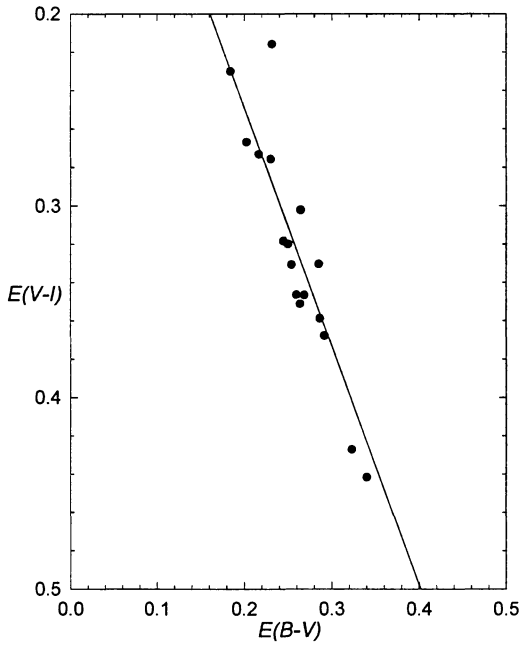

Fig. 5. The $E(V-I)$ versus $E(B-V)$ diagram. The solid line represents the relation from Dean et al. (1978) with a slope of 1.24.

think of them as members of the brightest part of a very reddened cluster seen through Trumpler 21 but, again, more observations are needed to prove this hypothesis.

4. DISTANCE AND AGE

The distance to Trumpler 21 was estimated by fitting the Schmidt-Kaler's (1982) ZAMS to the main sequence of the de-reddened cluster. The best fit in both the V_0 versus $(B-V)_0$ and V_0 versus $(U-B)_0$ planes, yielded $V_0 - M_V = 10.70 \pm 0.20$ corresponding to a distance of $d = 1380 \pm 100$ pc. This modulus was used to transform the V_0 magnitudes into absolute magnitudes, M_V. The disagreement with the modulus 10.90 from MF73 arises from a systematic 0.08 magnitude difference in V, but the disagreement with PF88 —who found 10.52— cannot be explained in this way because our data and theirs show a small systematic ΔV difference and similar mean reddenings. In this case the difference comes from an improved definition on our part of the lower main sequence which allowed for a more accurate ZAMS's fitting.

Figure 6 shows the M_V versus $(B-V)_0$ plane where the Schmidt-Kaler's (1982) ZAMS is fitted to $V_0 - M_V = 10.70$ and the isochrones computed from models with mass loss and overshooting developed by Schaller et al. (1992). We have found that the best isochrone fit including the two evolved members, stars # 1 and # 2, comes from the isochrones at 25 and 30 Myr. We adopt said values as the age limits of Trumpler 21.

5. POLARIZATION

As shown in Figure 7, the polarization data for 13 stars (given on Table 3) have been fitted with the standard Serkowski's law. (1973)

$$P_\lambda / P_{\max} = exp[-k \times \ln^2(\lambda_{\max}/\lambda)]\,,$$

where $k = 1.15$ was adopted. On doing this fitting we obtained the wavelength ($\lambda_{\max}$) at which maximum polarization ($P_{\max}$) occurs. The respective values for each star are also listed in Table 3.

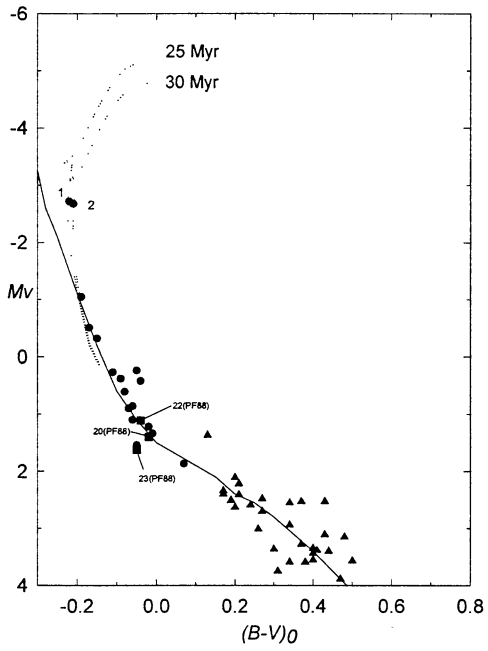

Fig. 6. The H-R diagram of likely and probable members of Trumpler 21. Solid line represents the Schmidt-Kaler's (1982) ZAMS fitted using a distance modulus of 10.7. Dotted lines are the isochrones from Schaller et al. (1992), their corresponding ages being indicated.

Although stars #6 and #20 have been classified as non-members of Trumpler 21 based on their position in the color-color and color-magnitude diagrams, no difference in polarization when compared to the member stars is seen. From Table 3 and Figure 7, star # 22 (in PF88 numbering) has low polarization in comparison with other cluster members and, like star # 19 and # 9, its wavelength of maximum polarization is rather blue. We also notice that stars # 22 from PF88, # 23 from PF88, and # 19 are poorly fitted by Serkowski's law. Apart from measurement errors, these stars may have intrinsic polarization. The overall normalized polarimetric wavelength dependence of the star sample is given in Figure 8. If we ignore cases of intrinsic polarization, the agreement with the standard Serkowski's law is reasonably good and suggests that polarization in the direction of Trumpler 21 is produced by interstellar dust. To reinforce this, the amount of polarization vectors and their position angle shown in Figure 9 indicate that, on average, they coincide with the general trend in the neighborhood of Trumpler 21, as shown in Klare & Neckel's catalogue (1977).

Figure 10 depicts the $P_{\max}$ versus $E(B-V)$ diagram. That is, the ratio of the maximum amount of polarization to the visual absorption. No star in this figure is located above the solid line which marks the empirical limit (Hiltner 1956).

$$P_{\max} < 3 \times A_V \approx 3 \times R \times E(B-V).$$

This diagram supports the idea of an interstellar origin for the stellar polarization as this limit cannot be exceeded when diffuse interstellar material, made up of normal-size grains having medium polarization efficiency, is acting.

The average wavelength at maximun polarization and average maximun polarization are $\overline{\lambda}_{\max} = 0.57 \pm 0.06$ μm and $\overline{P}(\lambda_{\max}) = 1.4 \pm 0.37\%$. This wavelength agrees with the typical one for the interstellar medium (0.545 μm; Orsatti, Vega, & Marraco 1998). Polarization can also be used to estimate the R value. According to Whittet & van Breda (1978), the R value depends on the wavelength at which the maximum polarization is achieved. This is

$$R = (5.6 \pm 0.3) \times \overline{\lambda}_{\max}.$$

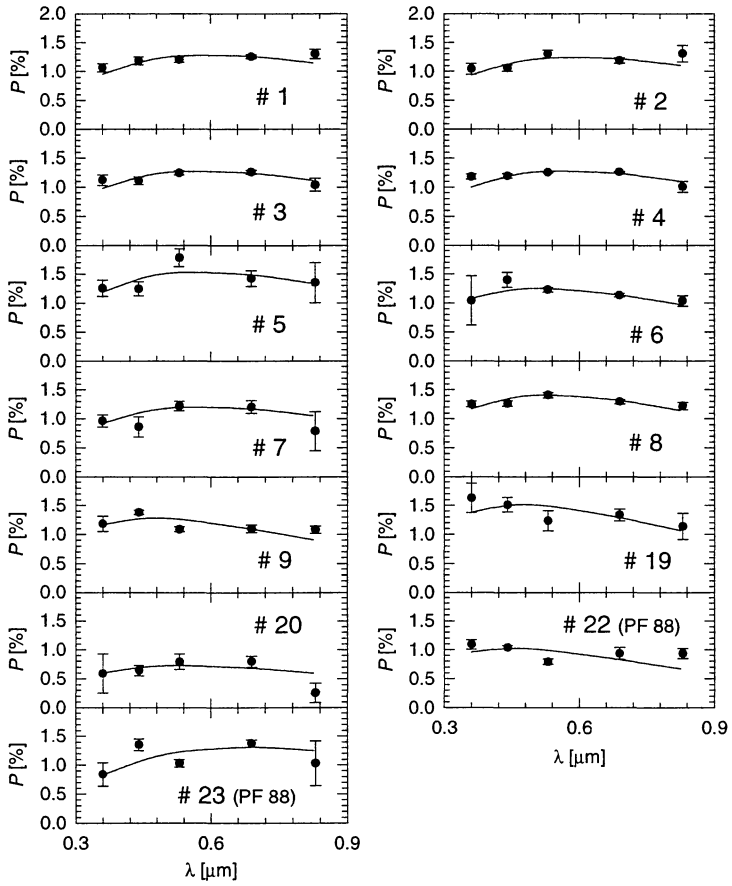

Fig. 7. Serkowski's law fit for 13 stars.

In our case, adopting $\overline{\lambda}_{\max} = 0.57\ \mu$m, we found $R = 3.17 \pm 0.3$, in close agreement with the 3.1 value estimated from photometry alone.

Let us briefly introduce a comment concerning supernova remnants around Trumpler 21. The catalogue of supernova remnants (SNRs) constructed by Whiteoak & Green (1996) lists three of these objects, G309.2–0.6, G308.1–0.7 and G308.7+00; the first two located 40′ west of the cluster and the latter, 70′. From our observations, no interaction between Trumpler 21 and these SNRs is evident. According to Seab & Shull's (1983) models, had supernova blast waves passed through the cluster, grain destruction would have taken place. As blast waves tend to destroy large grains preferentially, a notorious lowering in the average $E(B-V)$ and accordingly, an R value larger than 3.1 should have been detected. However, neither photometric nor polarimetric data confirm any different value, which suggests no interaction between the cluster and the SNRs.

6. CLUSTER MASS SPECTRUM

Cluster mass spectrum describes the distribution of stars in mass intervals. In particular, if such a description is referred to the moment of the cluster formation, it is called initial mass function. The cluster mass spectrum slope, assuming a power law (e.g., Scalo 1986), is given by

$$x = \log(dN/d(\log(M)))/\log(M)\ ,$$

where $dN/d(\log(M))$ is the number of stars having a mass M.

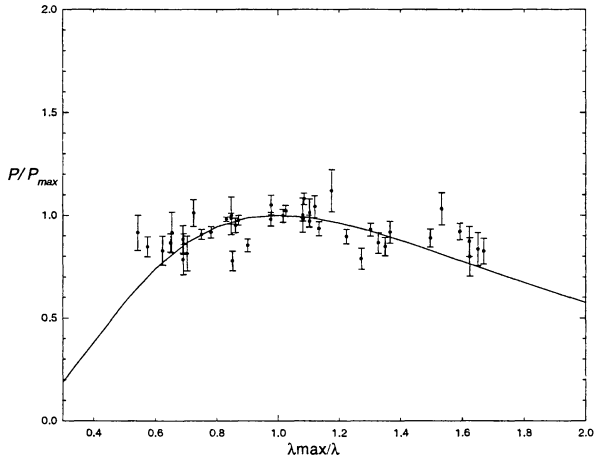

Fig. 8. Normalized polarimetric wavelength dependence for 13 stars observed in Trumpler 21.

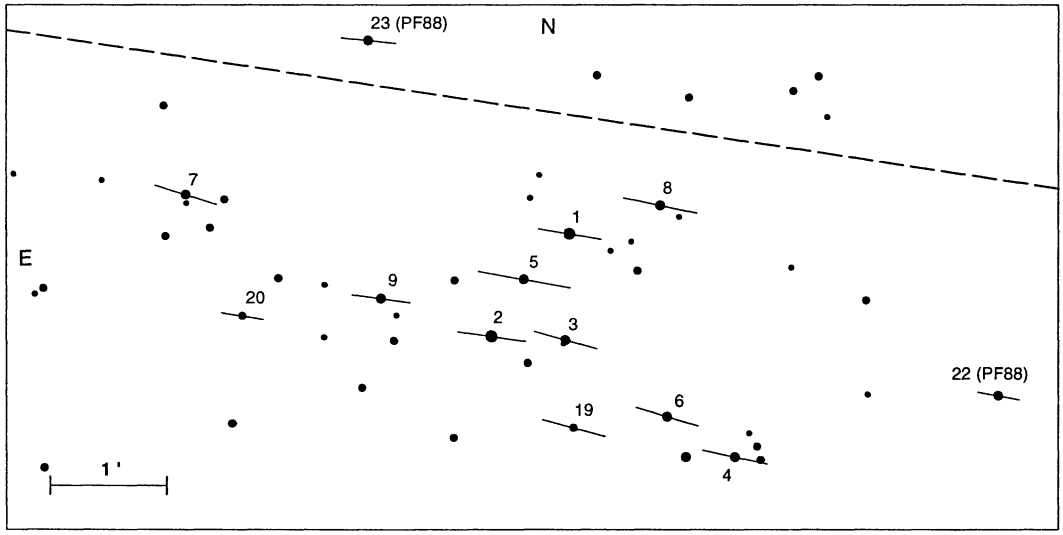

Fig. 9. The polarization vectors in Trumpler 21. Vectors superposed to each stars have a length and an orientation proportional to the polarization measured here. The dashed line is parallel to the galactic plane.

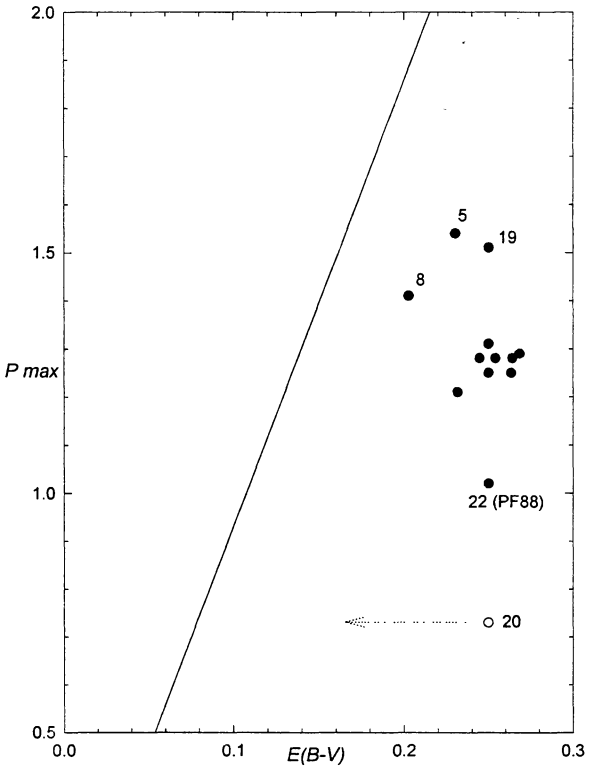

Fig. 10. $P_{\max}$ versus $E(B-V)$ relation. The line is the empirical limit of Hiltner (1956): $P_{\max} < 3 \times A_V$. Star # 20 was placed using the cluster average $E(B-V) = 0.25$. As it is likely to be suffering a lower reddening since it is not a member, its location should move as the arrow shows.

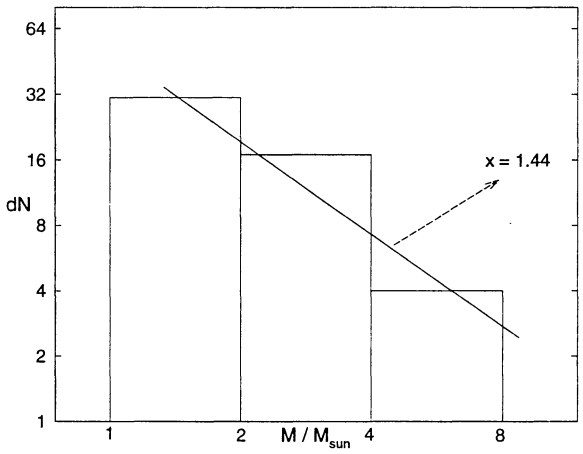

Fig. 11. The mass spectrum of Trumpler 21 (likely and probable members). The solid line represents the least squares fitting with a slope of 1.44.

Stellar masses of likely and probable members were obtained by transforming their corrected data from the M_V versus $(B-V)_0$ plane to the $\log(L/L_\odot)$ versus $\log(T_{eff})$ plane where an interpolation procedure was carried out using the evolutionary tracks of Schaller et al. (1992). The stars with spectroscopic classification were transformed using this information instead of their color indices. In all the cases, bolometric corrections were taken from Schmidt-Kaler (1982) as described in Vázquez et al. (1995). For three of the stars with known spectral types we found that the differences between our mass values and those expected from the mass-spectral type relation (Schmidt-Kaler 1982) were lower than 10%. However, star # 3 (B2V) has a mass 50% lower than expected; its spectral type should probably be verified.

Stellar masses were distributed into the mass bins from 1 to 8 $M_\odot$ as shown in Figure 11. The resulting slope of the mass distribution, also shown in Fig. 11 was obtained through a unweighted least squares fitting. It yielded $x = 1.44 \pm 0.08$ which is not far from the standard Salpeter's (1955) value, $x = 1.35$. The 1.44 value fits very well into the Tarrab's (1982) scheme where clusters with ages from 2.2×10^7 yr to 3.6×10^7 yr show mass distribution slopes from 1.58 to 0.96, respectively. It is possible to estimate the observed total mass of this cluster by making a simple sum of stellar masses. In the case where we only considered the likely members, we obtained $\log(M_{total}) \approx 1.8$, in agreement with a previous determination of Battinelli, Brandimarti, & Capuzzo-Dolcetta (1994). When probable member masses are also included, the cluster's total mass value would rise to $\log(M_{total}) \approx 2.1$.

7. CONCLUSIONS

The open cluster Trumpler 21 was investigated down to $V \approx 19$. We confirmed that it is a moderate young cluster of 25–30 Myr located at 1380 pc in a low absorption zone (with $E(B-V) = 0.25 \pm 0.02$), north-east of the Coalsack. The zone around this cluster is rich in SNRs although evidence for a connection between them and the cluster could not be found from our polarimetric data. The reddening is not only low but also follows a normal law characterized by $R = 3.1$. Polarization measurements confirm this result. In addition, the respective vectors of polarization follow the general interstellar trend in this zone. Few stars show evidence of intrinsic polarization but further observations are required.

Cluster members were assessed down to $V \approx 15$. Contamination by field stars is expected downwards this limit but looking at our color and magnitude diagrams, it does not seem to be strong. Apart from this, a near parallel sequence below $V \approx 15$ is evident in our diagrams, belonging probably to a distant cluster beyond Trumpler 21. Finally, there are several stars that rise above the reddened ZAMS in the color-color diagram that are candidates to be affected by blanketting.

In the mass range $1 < M < 8\ M_{\odot}$, this is down to $V \approx 15$, the cluster mass spectrum has a slope of 1.44 ± 0.08, consistent with Salpeter's value (Salpeter 1955). This value is also in agreement with the scheme proposed by Tarrab (1982). The mass of the cluster (based upon likely members) is over 60 $M_{\odot}$ but it can reach more than 125 $M_{\odot}$ if probable members are included.

The authors are indebted to Dr. Garrison for the allocation of telescope time at UTSO. E. G. made this work while a grant from the Comisión de Investigaciones Científicas de la Provincia de Buenos Aires. G. B., R. A. V., and A. F. acknowledge the kind assistance of the CASLEO staff and the CONICET support. We also thank the useful comments from Lic. M. Arias.

REFERENCES

Battinelli, P., Brandimarti, A., & Capuzzo-Dolcetta, R. 1994, A&AS, 104, 379
Cousins, A. W. J. 1978, Mon. Not. R. Astron. Soc. S.Afr., 37, 62
Dean, J. F., Warren, P. R., & Cousins, A. W. J. 1978, MNRAS, 183, 569
ESA 1997, The *Hipparcos* and *Tycho* Catalogues, ESA SP-1200
FitzGerald, M. P., Luiken, M., Maitzen, H. M., & Moffat A. F. J. 1979, A&AS, 37, 345
Gliese, W. 1969, Catalogue of Nearby Stars (Veroffentlichungen des Astronomischen Rechen-Instituts, Heidelberg), 22
Greenstein, J. L. 1965, in Galactic Structure, eds. A. Blaauw & M. Schmidt (Chicago: Univ. of Chicago Press), 361
Grotues, H.-G., & Gocherman, J. 1992, The Messenger, 68, 43
Hiltner, W. A. 1956, ApJS, 1, 389
Houk, N., Cowley, A. P., & Smith-More, M. 1975, The University of Michigan Catalogue of two-dimensional Spectral Types for the HD stars (Ann Arbor: Univ. of Michigan)
Hsu, J. C., & Breger, M. 1982, ApJ, 262, 732
Klare, G., & Neckel, Th. 1977, A&AS, 27, 215
Kumar, C. K. 1978, AJ, 219, L13
Moffat, A. F. J., & Vogt, N. 1973, A&AS, 10, 135
Orsatti, A. M., Vega, E., & Marraco, H. G. 1998, AJ, 116, 266
Peterson, C. J., & FitzGerald, M. P. 1988, MNRAS, 235, 1439
Salpeter, E. E. 1955, ApJ, 121, 161
Scalo, J. M. 1986, Fund. Cosm. Phys., 11, 1
Schaller, G., Schaerer, D., Meynet, G., & Maeder, A. 1992, A&AS, 96, 269
Schmidt-Kaler, Th. 1982, in Landolt-Bornstein VI/2b
Seab, C. G., & Shull, J. M. 1983, ApJ, 275, 652
Serkowski, K. 1973, in IAU Symp. 52, Interstellar Dust and Related Topics, eds. J. M. Greenberg & H. C. van der Hulst (Dordrecht: Reidel), 145
Serkowski K., Mathewson, D. S., & Ford V. L. 1975, ApJ, 196, 261
Stetson, P. 1987, PASP, 99, 191
Tarrab, I. 1982, A&A, 109, 285
Vázquez, R. A., Baume, G., Feinstein, A., & Prado, P. 1994, A&AS, 106, 339
Vázquez, R. A., Will, J.-M., Prado P., & Feinstein, A. 1995, A&AS, 111, 85
Whiteoak, J. B. Z., & Green A. J. 1996, A&A, 118, 329
Whittet, D. C. B., & van Breda, I. G. 1978, A&A, 66, 57

G. Baume, A. Feinstein, E. E. Giorgi, and R. A. Vázquez: Observatorio Astronómico de La Plata, Paseo del Bosque s/n, 1900 La Plata, Argentina (egiorgi@fcaglp.fcaglp.unlp.edu.ar).

TABLE 1

CCD PHOTOMETRIC OBSERVATIONS IN TRUMPLER 21[a]

#	PF88	X	Y	V	$(B-V)$	$(U-B)$	$(V-I)$	Remarks[b]
1	1	642.53	337.14	8.81	0.05	−0.58	0.12	lm HD 117492
2	2	552.91	219.90	8.84	0.06	−0.54	0.14	lm HD 117513
3	3	637.66	215.72	10.41	0.05	−0.48	0.13	lm
4	10	830.23	82.29	10.98	0.08	−0.39	0.17	lm
5	4	590.07	285.05	11.09	0.08	−0.34	0.13	lm
6	9	753.01	128.26	11.45	1.09	0.92	1.46	nm
7	7	205.16	381.98	11.68	0.12	−0.17	0.12	lm
8	8	745.54	370.04	11.70	0.11	−0.11	0.19	lm
9	5	426.55	263.07	11.76	0.21	0.09	0.26	lm
10	14	774.35	82.28	11.88	0.10	−0.08	0.16	lm
11	6	310.28	286.38	12.01	0.24	0.13	0.33	lm
12	11	719.66	294.72	12.37	0.20	0.05	0.30	lm
13		855.95	94.09	12.42	0.41	0.15	0.58	nm
14	12	510.47	283.67	12.60	0.25	0.06	0.37	lm
15		896.79	500.80	12.70	0.23	0.07	0.32	lm
16		859.40	78.60	12.71	0.20	0.14	0.27	lm
17	19	778.40	493.27	12.80	0.61	0.03	0.85	nm
18		43.47	70.06	12.80	0.27	0.18	0.32	lm
19	16	647.13	115.55	12.85	0.38	0.18	0.51	pm
20	17	269.66	243.00	12.86	0.56	−0.10	0.85	nm
21	20	673.72	518.84	13.05::	0.21::	0.06::	0.70::	lm**
22		249.53	376.49	13.06	0.47	0.17	0.64	nm
23		42.33	274.74	13.09	0.60	0.22	1.01	nm
24		180.55	483.86	13.17	0.47	0.16	0.62	nm
25	13	594.65	189.41	13.30	0.29	0.15	0.40	lm
26	15	509.82	104.10	13.34	0.32	0.20	0.40	lm
27		925.53	517.58	13.58	0.45	0.11	0.68	pm
28		182.08	334.33	13.69	0.46	0.18	0.66	pm
29		979.96	260.89	13.81	0.42	0.17	0.74	pm
30		258.13	120.05	13.87	0.42	0.27	0.57	pm
31		233.00	343.85	13.88	0.46	0.19	0.61	pm
32		441.56	214.62	13.95	0.52	0.18	0.73	pm
33	18	405.89	160.84	13.98	0.44	0.18	0.63	pm
34		444.31	243.60	14.00	0.68	0.16	1.11	pm
35		894.73	298.61	14.00	0.62	0.10	1.09	pm
36		635.46	211.74	14.03	0.59	0.26:	0.84	pm
37		109.12	398.80	14.07	0.49	0.13	0.66	pm
38		689.08	317.74	14.10	0.45	0.14	0.65	pm
39		8.59	405.88	14.17	0.52	0.10	0.69	pm
40	21	607.43	404.39	14.19	0.52	0.01	0.91	nm
41		712.68	328.37	14.22	2.13	0.81::	3.17	nm
42		362.31	218.78	14.28	0.67	0.48	1.08	nm
43		981.88	153.41	14.37::	−1.17::	−0.61::		nm
44		362.68	278.61	14.41	0.59	0.13	0.81	pm
45		846.82	108.98	14.48	0.51	0.21	0.77	pm
46		596.70	378.44	14.59	0.68	0.00	0.97	pm
47		206.11	372.15	14.60	0.78	0.45	1.24	nm
48		935.49	471.08	14.63	0.73	0.17:	1.07	pm
49		32.47	268.31	14.67	0.97	0.08	1.55	nm
50		767.02	356.59	14.74	0.49	0.02	0.73	nm
51		403.46	163.92	14.75	0.62	0.11	0.86	pm
52		493.93	237.15	14.83	0.65	−0.02:	0.97	pm
53		501.33	182.98	14.83	0.55	0.28:	0.93	pm

TABLE 1 (CONTINUED)

#	PF88	X	Y	V	$(B-V)$	$(U-B)$	$(V-I)$	Remarks[b]
54		800.69	185.83	14.85	0.67	0.03	0.93	pm
55		37.78	86.82	14.86	0.66	0.18	0.89	pm
56		41.34	222.79	14.88	0.69	0.14	0.90	pm
57		523.56	512.53	14.90	0.65	0.00:	0.88	pm
58		942.70	379.43	14.97	0.54	0.07:	0.80	nm
59		373.48	67.25	15.02	0.83	0.50	1.31	nm
60		147.74	287.19	15.03	0.65	0.14	0.91	pm
61		387.85	284.87	15.04	0.75	0.21	1.05	pm
62		574.84	94.85	15.06	0.63	0.22:	0.90	pm
63		188.20	227.40	15.07	0.59	0.13	0.80	pm
64		488.72	453.30	15.11	0.79	0.22::	1.04	
65		694.60	209.15	15.14	0.56	0.25::	0.95	
66		606.92	323.18	15.17	0.64	−0.13::	0.91	
67		698.34	145.79	15.22	0.56	0.11:	0.84	pm
68		762.37	254.30	15.27	0.64	0.01::	0.97	
69		859.01	189.28	15.27	1.55		2.35	
70		938.68	230.04	15.28	0.67	0.18::	0.94	
71		785.65	363.10	15.28	0.92	0.53::	1.25	nm
72		715.56	186.05	15.34	0.66	0.04:	0.94	nm
73		201.78	303.19	15.36	0.72	0.13	0.99	pm
74		874.84	356.18	15.39	0.74	0.44::	1.38	
75		166.21	388.77	15.40	0.96	0.84	1.23	nm
76		851.67	251.39	15.47	1.13		1.92	
77		689.18	247.10	15.54	0.92	0.64::	1.55	nm
78		923.17	342.52	15.55	0.88	0.02::	1.32	nm
79		174.47	82.72	15.55	0.95	0.29	1.61	
80		321.50	163.40	15.55	2.35	−0.07	4.03	nm
81		404.91	62.10	15.57	1.58	1.50:	2.23	nm
82		479.75	510.37	15.65	0.70		1.06	
83		282.20	8.77	15.68	0.85	0.38	1.14	
84		921.98	362.80	15.75	0.82		1.31	
85		784.99	111.18	15.77	0.65	−0.12::	0.97	nm
86		569.58	312.06	15.79	1.65		2.45	
87		283.98	71.53	15.82	0.91	0.44	1.41	
88		445.69	192.06	15.84	2.49		3.84	
89		264.92	348.44	15.85	0.78	0.18	1.10	
90		170.68	337.52	15.87	0.87	0.39	1.10	
91		417.71	138.76	15.90	0.90	0.47	1.20	
92		412.00	182.49	15.91	1.30	0.53	2.12	nm
93		95.93	141.41	15.91	0.84	0.42	1.42	
94		536.29	141.48	15.95	0.68	0.36::	0.98	
95		668.86	491.15	15.97	0.98		1.50	
96		897.49	282.54	15.97	0.91		1.32	
97		345.37	160.89	16.01	0.80	0.30	1.13	
98		286.19	339.17	16.03	0.83	0.40	1.18	
99		112.95	168.61	16.03	2.07		3.06	
100		726.08	104.91	16.10	0.84		1.46	
101		761.57	437.13	16.10	2.14		3.25	
102		1.67	336.38	16.11	0.88		1.43	
103		414.27	294.59	16.15	0.86	0.38	1.38	
104		709.17	295.25	16.16	0.80		1.11	
105		486.29	325.47	16.23	1.76		2.64	
106		899.40	225.88	16.24	1.19		1.98	
107		978.73	379.17	16.25	1.36		2.00	
108		903.73	503.76	16.25	0.99		1.45	

TABLE 1 (CONTINUED)

#	PF88	X	Y	V	$(B-V)$	$(U-B)$	$(V-I)$	Remarks[b]
109		613.04	396.13	16.26	1.60		2.43	
110		704.47	494.87	16.28	0.97		1.39	
111		300.46	202.32	16.32	1.17	1.00:	1.66	
112		548.22	49.97	16.34	0.72		1.00	
113		98.60	120.92	16.35	1.05	0.53	1.68	
114		289.70	252.49	16.36	1.02	0.40	1.50	
115		755.20	164.52	16.37	1.04		1.75	
116		514.75	263.47	16.41	1.79		2.48	
117		504.64	51.96	16.41	1.03		1.67	
118		591.15	211.26	16.41	0.87		1.56	
119		814.38	382.62	16.43	0.85		1.15	
120		586.41	89.73	16.43	1.84		2.72	
121		78.90	206.59	16.44	0.91	0.46	1.24	
122		281.08	220.31	16.48	1.75		2.49	
123		306.56	442.70	16.48	0.91	0.62:	1.22	
124		484.68	471.98	16.52	1.69		2.57	
125		42.12	377.20	16.59	0.89	0.54	1.21	
126		218.42	342.87	16.59	1.00	0.79:	1.33	
127		273.80	347.45	16.60	0.91	0.38	1.19	
128		254.39	20.83	16.61	1.40		2.05	
129		531.04	99.92	16.62	0.99		1.51	
130		960.50	419.76	16.63	0.91		1.44	
131		685.33	303.75	16.63	1.11		2.42	
132		565.56	476.96	16.64	0.92		1.26	
133		835.80	151.93	16.67	0.88		1.21	
134		356.93	331.05	16.67	1.04	0.62	1.47	
135		533.72	406.03	16.67	0.95		1.34	
136		425.02	162.69	16.68	0.85	0.40:	1.33	
137		763.51	364.52	16.69	0.91		1.54	
138		561.26	427.33	16.71	0.96		1.51	
139		973.71	326.52	16.72	1.24		1.69	
140		156.42	141.17	16.73	0.94	0.33:	1.23	
141		683.93	278.17	16.74	0.77		1.15	
142		818.47	158.70	16.77	1.06		1.43	
143		811.67	400.87	16.78	0.88		1.24	
144		10.75	397.45	16.80	0.84		1.12	
145		569.12	50.82	16.81	0.93		1.48	
146		365.48	405.04	16.82	1.26	0.51::	2.03	
147		496.88	133.31	16.82	1.15		1.72	
148		869.24	443.62	16.83	1.11		1.93	
149		741.09	375.21	16.83	1.18		2.08	
150		332.12	339.41	16.84	1.88		2.80	
151		432.08	313.68	16.85	1.32	0.71::	1.07	nm
152		208.20	199.91	16.85	1.09		1.73	
153		731.69	226.36	16.86	1.96		2.86	
154		698.83	201.97	16.87	0.80		1.16	
155		565.51	380.68	16.88	0.86		1.48	
156		924.75	465.91	16.90	1.05		1.67	
157		771.49	437.87	16.90	1.20		1.92	
158		123.87	283.89	16.91	1.98		2.89	
159		505.72	45.39	16.95	1.15		1.78	
160		910.08	441.78	16.96	0.90		1.23	
161		631.56	515.41	16.99	1.18		1.87	
162		909.38	405.47	16.99	1.00		1.53	
163		273.56	425.98	16.99	1.10		1.60	

TABLE 1 (CONTINUED)

#	PF88	X	Y	V	$(B-V)$	$(U-B)$	$(V-I)$	Remarks[b]
164		946.08	92.25	16.99	0.94		1.31	
165		157.42	338.58	17.00	0.94	0.56:	1.50	
166		943.97	385.87	17.03	0.92		1.40	
167		372.97	147.12	17.04	1.64	0.27::	2.80	nm
168		208.11	31.99	17.05	0.99		1.33	
169		259.04	136.49	17.06	1.08		1.78	
170		279.05	286.39	17.10	1.93		2.86	
171		489.01	107.60	17.10	1.33		2.21	
172		627.86	123.17	17.11	1.11		1.65	
173		43.22	472.26	17.13	1.00	0.65::	1.55	
174		271.09	286.51	17.13	0.96		1.45	
175		441.23	34.13	17.14	1.07		1.44	
176		835.40	105.29	17.14	0.76		1.19	
177		450.46	402.39	17.15	1.92		3.18	
178		873.24	339.37	17.16	0.98		1.36	
179		863.37	24.55	17.23	1.01		1.45	
180		434.91	63.48	17.25	1.95		3.00	
181		732.01	38.92	17.25	1.12		1.54	
182		562.67	158.11	17.25	0.96		1.55	
183		379.74	173.71	17.28	1.26		1.91	
184		868.25	314.17	17.28	1.18		1.49	
185		159.30	230.97	17.30	1.14	0.68::	1.75	
186		937.23	295.48	17.33	1.01		1.27	
187		874.70	166.30	17.34	2.16		3.22	
188		398.53	142.83	17.35	1.11	0.61::	1.54	
189		287.45	363.29	17.35	1.41		2.06	
190		655.62	136.27	17.36	1.60		2.57	
191		93.48	159.61	17.36	1.17		1.85	
192		51.70	489.45	17.36	1.16		1.84	
193		247.11	307.02	17.40	1.81		3.26	
194		427.48	344.97	17.44	1.05	0.25::	1.60	
195		22.65	394.75	17.44	2.02		3.45	
196		825.14	397.94	17.48	0.93		1.38	
197		897.78	198.05	17.50	0.99		1.46	
198		533.34	454.30	17.50	2.06		3.08	
199		583.98	54.93	17.54	0.94		1.28	
200		973.10	44.36	17.56	1.28		2.02	
201		425.07	125.69	17.59	1.02		1.64	
202		522.02	372.73	17.59	2.17		3.30	
203		403.50	125.38	17.60	1.06		1.38	
204		764.26	282.78	17.60	1.00		1.58	
205		186.02	384.05	17.60	0.74		1.28	
206		490.59	199.17	17.62	2.24:		3.13	
207		934.69	29.91	17.62	1.29		1.99	
208		15.42	175.82	17.63	1.37		1.98	
209		717.40	502.89	17.65	1.31		2.14	
210		949.49	274.31	17.66	2.09		3.23	
211		900.78	442.27	17.66	1.11		1.78	
212		181.73	444.67	17.67	1.10	0.27::	1.56	
213		559.62	127.08	17.68	1.36		1.91	
214		427.88	294.38	17.70	1.29		2.22	
215		852.68	30.77	17.71	1.20		1.91	
216		323.70	352.39	17.73	1.14		1.68	
217		221.92	168.42	17.76	1.06		1.42	
218		364.45	364.28	17.77	1.18		1.71	

TABLE 1 (CONTINUED)

#	PF88	X	Y	V	$(B-V)$	$(U-B)$	$(V-I)$	Remarks[b]
219		87.20	227.37	17.77	1.33		1.94	
220		428.47	305.15	17.77	1.01	0.49::	1.60	
221		294.05	389.80	17.79	1.17		1.96	
222		588.26	174.02	17.80	0.80		1.60	
223		108.86	205.87	17.80	1.23		1.85	
224		280.20	176.13	17.81	1.11:		1.55	
225		252.00	348.91	17.82	1.36:		2.02	
226		37.85	444.75	17.84	1.11		1.45	
227		858.64	494.12	17.84	1.22		1.87	
228		61.49	434.71	17.85	1.19		1.71	
229		339.40	7.25	17.86	0.98		1.51	
230		195.86	337.12	17.87	1.44:		1.98	
231		544.37	493.58	17.87	1.52		2.26	
232		802.74	503.03	17.88	1.11		1.68	
233		754.21	36.24	17.89	1.50		2.41	
234		512.48	443.82	17.91	1.25		1.72	
235		350.28	223.18	17.92	1.35		2.01	
236		49.76	407.63	17.92	1.13		1.83	
237		647.23	254.42	17.92	1.32		2.30	
238		788.26	130.35	17.93	1.55		2.27	
239		939.02	392.56	17.93	1.12		1.63	
240		467.51	186.89	17.94	1.04		1.30	
241		827.41	273.68	17.94	2.04:		3.13	
242		161.75	481.07	17.95	1.92:		3.56	
243		99.64	259.49	17.95	1.16		1.75	
244		587.69	467.89	17.96	1.29		2.29	
245		930.51	130.23	17.97	1.14		1.86	
246		178.48	378.69	17.97	1.16		1.93	
247		232.91	139.85	17.98	1.52		2.12	
248		268.40	454.24	17.99	1.08		1.66	
249		801.82	259.15	17.99	1.22::		1.86	
250		286.14	202.76	18.00	1.24		1.88	
251		804.99	239.15	18.01	1.28		2.04	
252		682.51	356.15	18.03	0.70:		1.65	
253		123.28	228.69	18.05	1.17		2.01	
254		954.75	247.73	18.05	1.38		1.86	
255		281.93	450.31	18.06	1.27		2.01	
256		550.29	445.58	18.06	1.24		1.95	
257		252.25	60.11	18.07	1.15		1.99	
258		144.31	224.73	18.09	2.16:		2.93	
259		146.21	413.02	18.11	1.17		1.83	
260		945.17	252.18	18.13	1.11		1.92	
261		706.58	174.25	18.14	1.07		1.66	
262		464.35	52.47	18.14	1.50:		2.36	
263		745.48	22.22	18.15	1.14		1.67	
264		188.51	179.53	18.17	1.13	0.22::	1.50	
265		661.14	234.36	18.17	0.95:		1.86	
266		169.20	295.15	18.18	1.26		2.13	
267		180.43	316.98	18.21	1.04:		1.54	
268		466.89	331.04	18.22	1.15		1.47	
269		977.64	221.63	18.23	1.22		2.01	
270		710.42	118.12	18.24	1.22		1.77	
271		673.47	414.43	18.25	1.04		1.96	
272		327.88	181.50	18.25	1.34		1.88	
273		627.47	294.57	18.25	0.65::		1.53	

TABLE 1 (CONTINUED)

#	PF88	X	Y	V	$(B-V)$	$(U-B)$	$(V-I)$	Remarks[b]
274		291.93	12.03	18.25	1.23		2.18	
275		189.53	249.51	18.26	1.20	1.67::	1.89	
276		662.22	483.86	18.26	1.10:		1.69	
277		775.51	228.74	18.26	1.65:		2.35	
278		884.50	213.25	18.27	1.05		1.92	
279		259.02	5.23	18.30	1.27:	0.24::	2.07	
280		417.07	79.48	18.30	1.17:		1.55	
281		752.19	80.57	18.31	0.75::		2.18	
282		446.64	226.65	18.31	1.29:		1.71	
283		954.76	80.12	18.31	1.55:		2.39	
284		755.57	89.18	18.32	0.61::		1.58	
285		377.81	453.26	18.34	1.22:		1.60	
286		747.05	184.07	18.34	1.30:		1.81	
287		823.59	21.06	18.36	1.25:		1.32	
288		61.30	22.01	18.36	1.29		1.75	
289		712.23	152.66	18.36	1.16::		2.01	
290		242.71	497.17	18.37	1.14		2.05	
291		974.85	390.20	18.38	1.03			
292		6.47	182.81	18.39	1.87::		3.36	
293		609.94	493.30	18.39	1.44:		2.16	
294		944.19	34.18	18.40	1.27:		2.07	
295		741.73	346.01	18.41	0.97:		2.07	
296		145.48	299.98	18.45	1.50::		2.30	
297		433.69	422.40	18.46	1.24:		1.93	
298		499.28	438.51	18.46	1.14		1.85	
299		652.43	499.30	18.47	1.24:		1.60	
300		867.77	290.15	18.49	2.29::		3.24	
301		255.75	468.69	18.50	1.29:		2.17	
302		892.08	45.87	18.51	1.18:		1.97	
303		958.39	436.54	18.52	1.24:		1.92	
304		338.41	466.70	18.53	1.21:		1.96	
305		278.80	388.86	18.53	0.92:		1.83	
306		697.19	383.37	18.53	1.06::		2.15	
307		453.02	262.11	18.54	0.93:		1.64	
308		542.46	22.53	18.55	1.55::		2.10	
309		574.04	341.92	18.56	1.42::		2.60	
310		377.79	479.88	18.57	1.09::		2.00	
311		743.64	320.77	18.57	1.10::		2.04	
312		139.86	229.00	18.58	1.28::		2.08	
313		806.13	231.95	18.60	1.56::		2.43	
314		550.30	277.24	18.60	1.75::		2.39	
315		609.44	102.30	18.62	1.43:		2.04	
316		107.78	86.69	18.62	1.60::		3.12	
317		93.86	204.19	18.63	1.20:		1.77	
318		656.87	168.60	18.64	1.00:		1.90	
319		634.13	464.58	18.64	1.27:		2.22	
320		660.72	161.66	18.65	1.75::		2.78	
321		140.95	434.84	18.66	1.54::		2.33	
322		438.16	430.20	18.66	1.45::		2.34	
323		617.57	415.73	18.66	0.93:		1.58	
324		49.07	361.34	18.67	1.15::		1.93	
325		378.31	210.70	18.67	1.63::		2.56	
326		727.05	76.40	18.68	1.22:		1.65	
327		357.50	453.39	18.69	1.37:		2.04	
328		941.30	245.19	18.70::	0.51::			

TABLE 1 (CONTINUED)

#	PF88	X	Y	V	$(B-V)$	$(U-B)$	$(V-I)$	Remarks[b]
329		307.73	389.29	18.70	1.40::		1.66	
330		938.16	306.75	18.71	1.31::		2.03	
331		769.32	115.53	18.74	1.70::		1.88	
332		472.73	22.05	18.74	1.28::		2.15	
333		173.50	211.83	18.75	1.40::		1.89:	
334		914.38	298.97	18.80	1.15::		1.80	
335		533.66	56.19	18.82	1.55::		2.32	
336		255.17	303.44	18.82	1.45::		1.94	
337		321.87	13.95	18.82	1.43::		2.07	
338		282.86	488.27	18.83	1.18::		2.15	
339		218.72	449.48	18.84	1.35::		1.75	
340		321.12	99.66	18.87	1.40::		2.04	
341		87.87	476.08	18.88	1.35::		2.15	
342		960.98	316.57	18.90	1.35::		2.23	
343		626.69	25.57	18.90	1.19:		1.87	
344		542.93	156.39	18.93	0.81::		1.55:	
345		680.15	56.91	18.94	1.29::		2.10	
346		759.84	177.44	18.95	1.34::		1.99	
347		470.63	171.90	18.98	1.09::		1.82	
348		896.05	327.90	18.98	1.31::		2.06	
349		907.94	379.03	19.00	1.35::		2.39:	
350		260.58	413.60	19.01	1.39::		2.25	
351		206.22	282.08	19.03	1.66::		2.40	
352		646.20	385.00	19.04::	−0.01::			
353		293.40	207.89	19.07::	1.07::		2.20::	
354		813.24	170.66	19.14	1.55::		2.14	
355		366.32	350.80	19.16	1.46::		2.41:	
356		853.00	262.21	19.20	1.66::		2.43	
357		24.42	5.85	19.20	1.18::		2.19:	
358		429.74	411.10	19.24	1.54::		1.85:	
359		223.56	259.01	19.30:	1.10::		2.06::	
360		519.85	419.20	19.33:	1.50::		2.29:	
361		497.88	378.30	19.35:	0.99::		2.88:	
362		348.94	126.92	19.50	0.95::		2.04:	
363		497.08	32.29	19.55:	1.10::		2.12:	
364		617.78	134.57	19.76::	2.13::		2.50::	
365		390.07	100.06	19.86::	2.01::			
366		548.51	113.73	19.90:	0.64::		1.89	
...	22			12.37	0.14	0.05		lm*
...	23			13.09	0.20	0.18		lm*

[a] We use the following notation: # = Sequence number, PF88 = number in PF88 notation, X = X position, Y = Y position, (:) errors larger than 0.07, (::) errors larger than 0.10.

[b]Remarks: lm = likely member, pm = probable member, nm = non member, * = data from PF88, ** = this star is located near the edge of our frame, then we use its data from PF88.